J Supercond Nov Magn (2014) 27:77–82
DOI 10.1007/s10948-013-2268-3

ORIGINAL PAPER

Evaluation of Microstructural and Mechanical Properties of Ag-Diffused Bulk MgB_2 Superconductors

M. Yilmazlar · C. Terzioglu · M. Dogruer · F. Karaboga · N. Soylu · Y. Zalaoglu · G. Yildirim · O. Ozturk

Received: 15 April 2013 / Accepted: 23 May 2013 / Published online: 7 June 2013
© Springer Science+Business Media New York 2013

Abstract Electrical, microstructural, and mechanical properties of undiffused and Ag-diffused bulk MgB_2 superconductors are systematically studied using dc resistivity, scanning electron microscopy (*SEM*), and Vickers microhardness (H_V) measurements. The resistivity (at room temperature), critical (onset and offset) temperature, variation of transition temperature, hole-carrier concentration, surface morphology, Vickers microhardness, elastic modulus, and yield strength values of the samples are obtained and compared with each other. One can see that all superconducting parameters given above depend on the Ag diffusion on MgB_2 system. The obtained results illustrate that the room temperature resistivity reduces with the increment of diffusion annealing temperature because of the hole filling when the onset (T_c^{onset}) and offset (T_c^{offset}) critical temperatures determined from the resistivity curves are obtained to enhance from 38.4 to 39.7 K and from 36.9 to 38.8 K, respectively. Further, SEM studies carried out for the microstructural characterization demonstrate that the surface morphology and grain connectivity also improve with the increase of the diffusion annealing temperature. In fact, the best surface morphology is observed for the Ag-diffused bulk MgB_2 superconductor exposed to 850 °C annealing temperature. Besides, it is obtained that the load-dependent microhardness values reduce nonlinearly as the applied load increases until 2 N, beyond which the curves shift to the saturation region, presenting that all the samples exhibit the indentation size effect (ISE) behavior. Further, the elastic modulus and yield strength values observed decrease with the enhancement of the applied load.

Keywords Ag diffused MgB_2 · Transition temperature · Scanning electron microscopy · Vickers microhardness

M. Yilmazlar
Department of Elementary Education, Sakarya University, Sakarya 54187, Turkey

C. Terzioglu (✉) · M. Dogruer · F. Karaboga · N. Soylu · Y. Zalaoglu
Department of Physics, Abant Izzet Baysal University, Bolu 14280, Turkey
e-mail: terzioglu_c@ibu.edu.tr

Y. Zalaoglu
Department of Physics, Osmaniye Korkut Ata University, Osmaniye 80000, Turkey

G. Yildirim
Department of Mechanical Engineering, Abant Izzet Baysal University, Bolu 14280, Turkey

O. Ozturk
Department of Physics, Kastamonu University, Kastamonu 37100, Turkey

1 Introduction

Magnesium diboride (MgB_2) superconducting material by Nagamatsu et al. [1] in 2001 exhibits the highest critical transition temperature, critical current density, and irreversibility field among the intermetallic compounds. Further, two conduction bands and two superconducting gaps in its structure have attracted great attention for the fundamental researches. The MgB_2 material is defined as 1.5-type superconductor due to the exhibition of both the type-I and type-II superconducting properties simultaneously [2]. In the last decade, some important characteristics belonging to the MgB_2 materials such as the incredible high intrinsic critical current density ($J_c > 10^7$ A/cm^2), light density (2.55 g/cm^3), simple chemical composition, low-cost preparation, simple crystal structure, low resistivity near T_c (0.4–

16 μΩ cm at 40 K), low anisotropy (≈5.4 at low temperature), large irreversibility field high upper critical field (14–39 T, perpendicular to the c-axis, $\mu_0 H \| ab$), high critical temperature (≈39 K), large coherence length, and absence of weak links have fostered the researchers to use these materials in potential applications in technology and industry [3–7]. In other words, the properties given above make the MgB_2 material an excellent candidate for the fundamental researches in the material science and practical applications. However, the purity as well as the applied magnetic field and high temperatures limit their applications seriously. Namely, the reaction complexity sometimes leads to the different phase appearances in the MgB_2 structure, such as MgB6, MgB12, and MgO, during the phase formation [8–11] due to the preparation conditions including the annealing ambient, composition, type and quantity of the chemicals. Thus, the superconducting properties such as critical transition temperature, critical current density, and irreversibility field degrade in the presence of the different phases discussed above in the structure. As is well known, several studies (chemical doping, substitution, and transition metal diffusion) on improvement of the superconducting properties of the bulk MgB_2 materials have been performed for years [12, 13]. Among the studies, the transition metal diffusion researches are the superior to others as a result of the reproducible and controllable mechanism at relatively low concentration level between 10^{16} and 10^{21} cm^{-3} [14, 15]. To our best knowledge, no detailed examination on the Ag-diffused bulk MgB_2 material has been published in the literature.

In the present work, we try to report the electrical, microstructural, and mechanical properties of undiffused and Ag-diffused bulk MgB_2 superconducting materials by means of the dc resistivity, scanning electron microscopy, and Vickers microhardness measurements. The dc resistivity measurements enable us to determine the room temperature resistivity, onset and offset critical transition temperatures, and variation of transition temperature when the SEM images allow us to investigate the specimen surface morphologies. Similarly, the elastic modulus and yield strength values that are in charge of the mechanical properties are also described by Vickers microhardness examinations. The findings obtained are clearly discussed in the results and discussion part.

2 Experimental Details

The undiffused and Ag-diffused bulk samples are prepared by the precursor powder of MgB_2 (Alfa Aesar, −325 mesh, >44 micron). The powder is pressed into rectangular bars of $40 \times 4 \times 2$ mm^3 with a pressure of 350 MPa and put in a tube furnace (Protherm-Model PTF12/75/200) under 5 bar argon gas pressures and sintered at 850 °C for 1 h. The heating and cooling rates of the temperature are adjusted to be 5 °C/min^{-1}. The Ag evaporation (thickness of about 30 μm) on one face of the samples is carried out via AUTO 306 vacuum coater (EDWARDS) under pressure of 2×10^{-5} Torr, and hence Ag diffusion is found through the samples. Then, the Ag evaporated superconducting samples are annealed at 650, 700, 750, 800, and 850 °C for 1 h. After the annealing processes, there were not found any residuals on the samples. Moreover, the dc resistivity measurements were conducted on the samples using the conventional four-probe method. We measured the temperature (25–45 K) dependence of resistivity of the sample running 5 mA DC current through the sample in the cryostat. A Keithley 220 programmable current source and a Keithley 2182A nanovoltmeter were used for the resistivity measurements. Further, microstructure observations were examined by using scanning electron microscope (SEM) JEOL 6390-LV, operated at 20 kV, with a resolution power of 3 nm.

3 Results and Discussion

3.1 Electrical Resistivity Measurements

The temperature dependence of the electrical resistivity for the samples produced in the temperature range 25–45 K to study the effect of Ag diffusion on superconducting properties of the samples and results obtained are shown in Fig. 1. As can be seen from the figure, all the samples illustrate metallic behavior above the onset critical temperature values. In other words, each sample demonstrates the superconducting feature below their variable offset critical temperature values. The normal state resistivity of the samples is obtained to reduce with the increment of the Ag nanoparticles in the MgB_2 matrix to a minimum (0.369 Ω m) for Ag5 sample as against 0.975 Ω m for the Ag0 sample (Table 1). This may stem from the fact that the excess inclusions begin to fill the holes in the crystal structure and so decrease in the normal-state resistivity is observed with increment of the diffusion annealing temperature. Further, the onset critical (T_c^{onset}) and offset critical (T_c^{offset}) temperature values, deduced from Fig. 1, are obtained to be in the ranges of 38.4–39.7 K and 38.8–36.9 K, respectively (Table 1). It is clear from Table 1 that both T_c^{onset} and T_c^{offset} values enhance with increasing the diffusion annealing temperature. The maximum critical temperature values ($T_c^{\text{onset}} = 39.7$ and $T_c^{\text{offset}} = 38.8$ K) are found for the Ag5 sample because of the improvement of the crystallinity and connectivity between grains. Besides, to obtain the important parameters about the MgB_2 superconductors, the variation of ΔT_c ($T_c^{\text{onset}} - T_c^{\text{offset}}$) value is gathered in Table 1. As can be seen from the table, the ΔT_c value reduces from 1.5 to 0.9 K

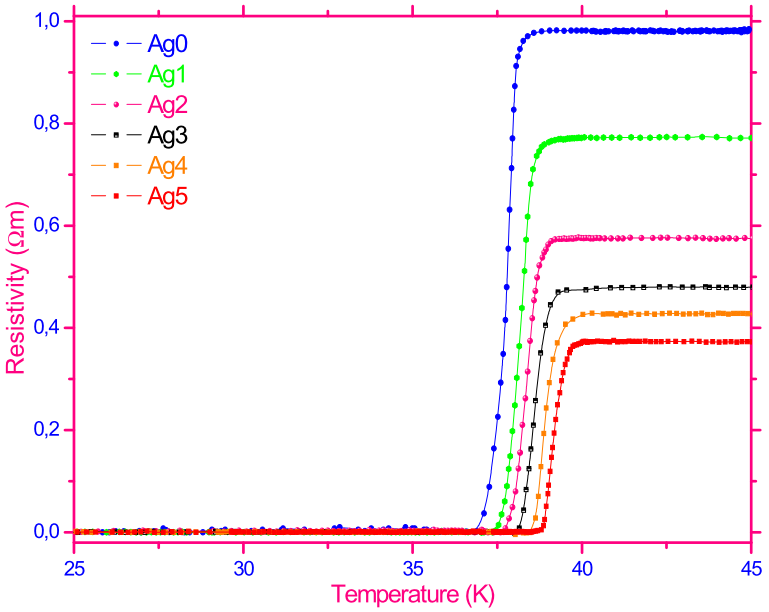

Fig. 1 Resistivity as a function of temperature curves for the samples

Table 1 Resistivity measurement results for the samples

Samples	T_c^{onset} (K)	T_c^{offset} (K)	ΔT_c (K)	$\rho_{300\text{K}}$ (Ω m)
Ag0	38.4	36.9	1.5	0.975
Ag1	38.8	37.4	1.4	0.765
Ag2	38.9	37.6	1.3	0.569
Ag3	39.3	38.1	1.2	0.466
Ag4	39.5	38.4	1.1	0.419
Ag5	39.7	38.8	0.9	0.369

with enhance of diffusion annealing temperature. This may be due to the increment of the crystallinity [16]. Especially, this decrement may be attributed to the divergence from the optimization of the hole concentration, being favored by the results of the SEM measurements [17–19]. According to this results obtained, the Ag5 sample is observed to be the best sample for the technology and industrial applications.

3.2 Microstructure Analyses

The surface morphologies of the pure and Ag-diffused bulk MgB_2 superconductors are studied by SEM, and the micrographs pictured are visualized in Fig. 2. It is obvious from the figure that not only the Ag foreigners inserted in the Bi-2223 system but also the diffusion annealing temperature make the microstructures (crystallinity, texturing, and porosity) of the samples change considerably. The dense surface with a fine connectivity between the grains improves with the increase of both the annealing temperature and the Ag inclusions in the MgB_2 matrix. Based on the figure, the specimen surface belonging to the bulk Ag0 sample is found to be the worst, roughest, and most porous with the characteristic appearance among the superconducting samples produced. On the other hand, the Ag5 sample obtains more uniform surface appearance with smoother and broader grain size distribution, lower porosity, higher density, and better texturing, crystallinity, alignment, and connectivity between the grains. The long and short of it is that the superconducting properties of the bulk MgB_2 samples improve with both the Ag inclusions and diffusion annealing temperature as a consequence of the elongation of the crystalline size leading to the better connectivity between the superconducting grains.

3.3 Microhardness and Modeling

In this study, the effect of the Ag nanoparticles on the mechanical performances of the MgB_2 systems by means of the measurement of the diagonal lengths in the applied load range from 0.245 N to 2.940 N and Vickers microhardness (H_V) values are calculated by use of the following equa-

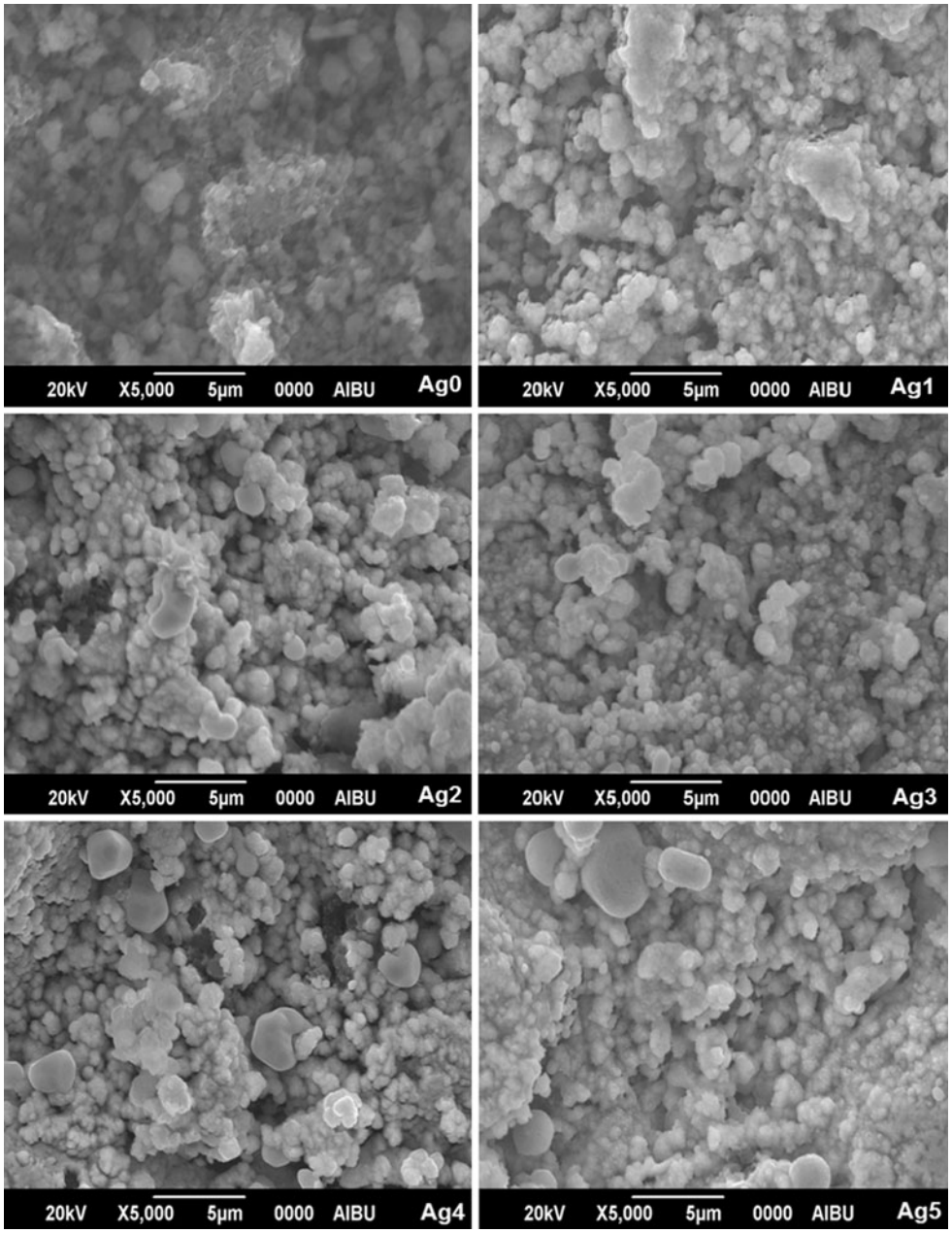

Fig. 2 SEM micrographs of undiffused and Ag-diffused samples

tion:

$$H_V = 1854.4\left(\frac{F}{d^2}\right) \tag{1}$$

where F presents the applied load, and d is the indentation diagonal lengths. The calculated load-dependent microhardness values (H_v) for different applied loads ($F = 0.245$, 0.490, 0.980, 1.960, and 2.940 N) are gathered in Table 2. As is seen from the table, the H_v values obtained strongly depend on both the diffusion annealing temperature and applied loads. It is visible from the table that the microhardness values of Ag5, Ag4, Ag3, Ag2, Ag1, and Ag0 samples at 2.940 N are 2.898, 2.186, 1.920, 1.328, 1.101, and 0.751 GPa, respectively. It is obtained that the load-dependent microhardness values increase with increasing annealing temperature from 650 to 850 °C. This may be attributed to the fact that the bonding strength enhances and therefore microhardness values are improved. The variation of microhardness versus the applied loads for all the samples is illustrated in Fig. 3. In the literature, the superconducting samples indicate two different features to identify as the indentation size effect (*ISE*) [20] and reverse indentation size effect (*RISE*) [21]. In this study, all the samples exhibit ISE behavior being attributed to the fact that the mi-

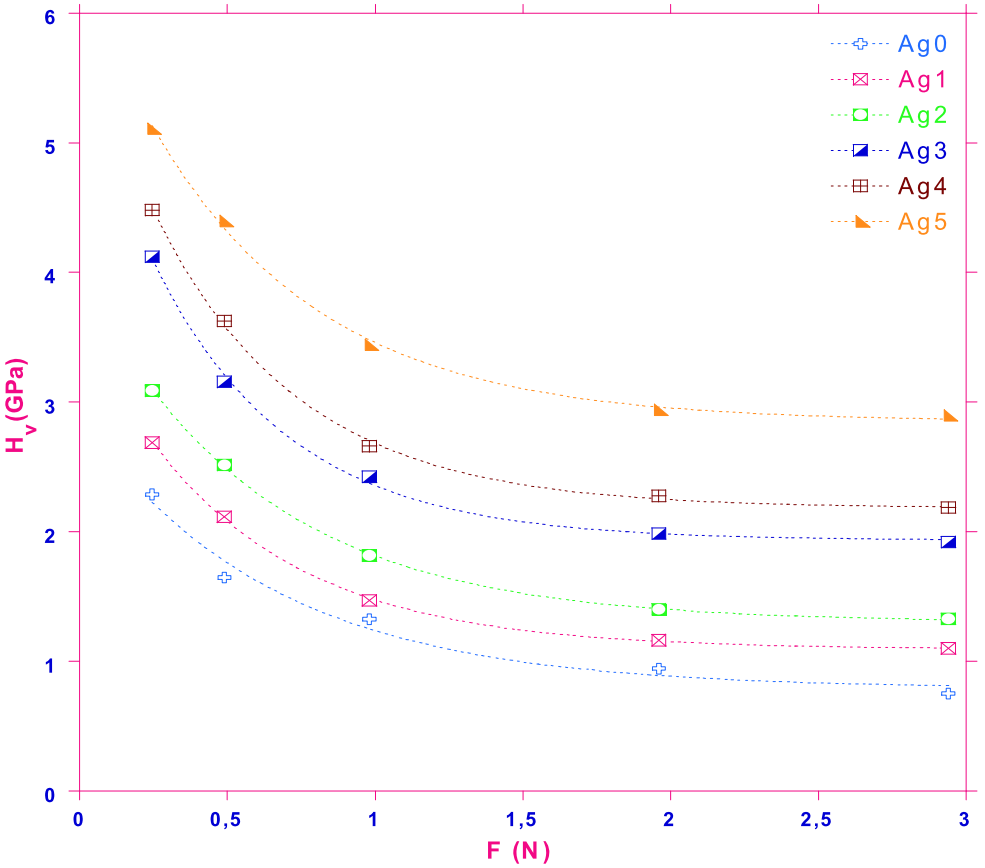

Fig. 3 Variation of load-dependent microhardness H_V as a function of different applied loads F for ISE behaviors

crohardness values decrease nonlinearly with increasing applied load from 0.245 N to 2.000 N; after this point a minor change is observed because of the shifting of the curves to saturation (nearly plateau) region. The change in the curves is owing to the grain boundary weak links, specimen cracking/porosity, disorder, impurity phases, and irregular grain orientation distribution [22]. Dogruer et al. [23] studied MgB_2 inclusions in Bi-2223 matrix. They obtained that the Vickers microhardness values increase with the increasing applied loads for $x = 0.01$, 0.03, and 0.05 samples and exhibit the reverse indentation size effect (RISE) behavior.

Furthermore, the elastic (Young's) modulus (E) and yield strength (Y) determined from the microhardness values can be calculated from the following equations:

$$E = 81.9635 H_V, \tag{2}$$

$$Y \approx \frac{H_V}{3}. \tag{3}$$

The obtained results are listed in Table 2. As can be seen from the table, all the results depend strongly on the Ag inclusions, applied load, and especially diffusion annealing temperature. One can see that the elastic modulus and yield strength obtained decrease (increase) with the enhancement of the applied load (annealing temperature) for all the samples.

4 Conclusions

From the above findings the following conclusions can be drawn:

- The normal state resistance of the samples increases with the increasing diffusion annealing temperature, owing to the decrease in the number of holes.
- Both the T_c^{onset} and T_c^{offset} values increase with increment of the diffusion annealing temperature.
- The ΔT_c value decreases with ascending diffusion annealing temperature, presenting the decrement of the crystallinity and grain connectivity.
- According to results of SEM investigations, the Ag5 sample shows the best surface morphology, best grain connectivity, and lowest porosity among the samples.
- The Vickers microhardness measurements for all samples exhibit the ISE behavior. The reason for this behavior is contribution of the grain boundary weak links, specimen cracking/porosity, disorder, impurity phases, and irregular grain orientation.

Table 2 The calculated H_V, E, and Y values for the samples

Samples	F (N)	d (μm)	H_V (GPa)	E (GPa)	Y (GPa)
Ag0	0.245	14.09	2.288	187.572	0.762
	0.490	23.50	1.645	134.860	0.548
	0.980	37.04	1.324	108.569	0.441
	1.960	62.05	0.944	77.374	0.314
	2.940	85.20	0.751	61.559	0.250
Ag1	0.245	13.00	2.688	220.345	0.896
	0.490	20.73	2.114	173.309	0.704
	0.980	35.14	1.471	120.627	0.490
	1.960	55.87	1.164	95.438	0.388
	2.940	70.36	1.101	90.265	0.367
Ag2	0.245	12.12	3.092	253.504	1.030
	0.490	19.00	2.517	206.306	0.839
	0.980	31.62	1.817	148.979	0.605
	1.960	50.91	1.402	114.940	0.467
	2.940	64.07	1.328	108.858	0.442
Ag3	0.245	10.49	4.128	338.406	1.376
	0.490	16.96	3.158	258.921	1.052
	0.980	27.36	2.427	198.983	0.809
	1.960	42.77	1.986	162.855	0.662
	2.940	53.28	1.920	157.413	0.640
Ag4	0.245	10.06	4.489	367.954	1.496
	0.490	15.82	3.630	297.582	1.210
	0.980	26.13	2.661	218.158	0.887
	1.960	39.96	2.276	186.564	0.758
	2.940	49.94	2.186	179.173	0.728
Ag5	0.245	9.43	5.109	418.761	1.703
	0.490	14.37	4.400	360.667	1.466
	0.980	22.98	3.44	282.065	1.147
	1.960	35.15	2.941	241.117	0.980
	2.940	43.37	2.898	237.570	0.966

- The Young modulus and yield strength values reduce with the increase of applied load for the all samples presenting the ISE nature and increase for all the samples with the diffusion annealing temperature.

References

1. Nagamatsu, J., Nakagawa, N., Muranaka, T., Zenitani, Y., Akimitsu, J.: Nature **410**, 63–64 (2001)
2. Dogruer, M., Zalaoglu, Y., Yildirim, G., Varilci, A., Terzioglu, C.: J. Mater. Sci., Mater. Electron. **24**, 958–967 (2013)
3. Golubov, A.A., Brinkman, A., Dolgov, O.V., Kortus, J., Jepsen, O.: Phys. Rev. B **66**, 054524 (2002)
4. Fletcher, J.D., Carrington, A., Taylor, O.J., Kazakov, S.M., Karpinski, J.: Phys. Rev. Lett. **95**, 097005 (2005)
5. Zehetmayer, M., Eisterer, M., Jun, J., Kazakov, S.M., Karpinski, J., Wisniewski, A., Weber, H.W.: Physica C **408**, 111–113 (2004)
6. Angst, M., Castro, D.D., Eshchenko, D.G., Khasanov, R., Kohout, S., Savic, I.M., Shengelaya, A., Bud'ko, S.L., Canfield, P.C., Jun, J., Karpinski, J., Kazakov, S.M., Ribeiro, R.A., Keller, H.: Phys. Rev. B **70**, 224513 (2004)
7. Bugoslavsky, Y., Perkins, G.K., Qi, X., Cohen, L.F., Caplin, A.D.: Nature **410**, 563–565 (2001)
8. Kolesnikov, N.N., Kulakov, M.P.: Physica C **363**, 166–169 (2001)
9. Pan, X.F., Zhao, Y., Feng, Y., Yang, Y., Cheng, C.H.: Physica C **468**, 1169–1173 (2008)
10. Ma, Z., Liu, Y.: Mater. Chem. Phys. **126**, 114–117 (2011)
11. Zhang, Y., Zhou, S.H., Wang, X.L., Dou, S.X.: Physica C **468**, 1383–1386 (2008)
12. Jin, S., Teifei, T.H., Sherwood, R.C., Davis, M.E., van Dover, R.B., Kammlott, G.W., Fasrnacht, R.A., Keith, H.D.: Appl. Phys. Lett. **52**, 2074–2076 (1988)
13. Salama, K., Selymanickam, V., Gao, L., Sun, K.: Appl. Phys. Lett. **54**, 2352–2354 (1989)
14. Hur, J.M., Togano, K., Matsumoto, A., Kumakura, H., Wada, H., Kimura, K.: Supercond. Sci. Technol. **21**, 032001 (2008)
15. Guclu, N.: J. Alloys Compd. **509**, 1691–1695 (2011)
16. Dogruer, M., Yildirim, G., Yucel, E., Terzioglu, C.: J. Mater. Sci., Mater. Electron. **23**, 1965–1970 (2012)
17. Ianculescu, A., Gartner, M., Despax, B., Bley, V., Lebey, Th., Gavrila, R., Modreanu, M.: Appl. Surf. Sci. **253**, 344–348 (2006)
18. Mangapathi Rao, D., Somaiah, T., Haribabu, V., Venudhar, Y.C.: Cryst. Res. Technol. **28**, 285–298 (1993)
19. Kocabas, K., Ozkan, O., Bilgili, O., Kadıoglu, Y., Yılmaz, H.: J. Supercond. Nov. Magn. **23**, 1485–1492 (2010)
20. Dogruer, M., Zalaoglu, Y., Gorur, O., Ozturk, O., Yildirim, G., Varilci, A., Yucel, E., Terzioglu, C.: J. Mater. Sci., Mater. Electron. **24**, 776–783 (2013)
21. Dogruer, M., Karaboga, F., Yildirim, G., Terzioglu, C., Ozturk, O.: J. Mater. Sci., Mater. Electron. (2013). doi:10.1007/s10854-013-1152-z
22. Ling, H.C., Yan, M.F.: J. Appl. Phys. **64**, 1307–1311 (1988)
23. Dogruer, M., Yildirim, G., Varilci, A., Terzioglu, C.: J. Alloys Compd. **556**, 143–152 (2013)